Journal of
Water & Climate Change

IWA PUBLISHING

Journal of Water and Climate Change Vol 13 No 2, 872 doi: 10.2166/wcc.2022.330

Estimation of greenhouse gas emissions of a tropical reservoir in Colombia

Diana C. Rodríguez* and Gustavo A. Peñuela

Pollution Diagnostics and Control Group (GDCON), Environment School, Faculty of Engineering, University Research Campus (SIU), University of Antioquia (UdeA), Calle 70 No. 52-21, Medellin, Colombia
*Corresponding author. E-mail: diana.rodriguez@udea.edu.co

DCR, 0000-0002-9310-6925; GAP, 0000-0003-3065-0285

ABSTRACT

Tropical reservoirs are generally flooded in soils with a high content of organic matter. This, combined with high temperatures, favors the generation of carbon dioxide and methane by biological degradation, contributing to the impact on climate change. A tropical reservoir in Colombia was monitored for 7 years in the pre-fill, fill and post-fill stages, for the last of these during the day and night. Emissions from diffusive fluxes at the surface of the water were measured using a floating static chamber, while inverted funnel methodology was used to measure the fluxes by bubbling. The samples collected in the field were analyzed in the laboratory using a gas chromatograph with a mass detector. The results showed average emissions of 70892.51 ± 41079.16-ton CO_{2eq}/year for pre-filling; 178254.53 ± 105838.01-ton CO_{2eq}/year for filling; and 466946.57-ton CO_{2eq}/year for post-filling (for 5 years), concluding that the weather conditions and the filling percentage had an impact on the generation of greenhouse gases at filling and post-filling stages, as did the organic matter present in the area of influence of the sampling point. Higher greenhouse gas emissions were found during the day compared to the results at night, indicating that temperature affects these processes especially in tropical reservoirs.

Key words: bubbling, diffusive fluxes, greenhouse gases, reservoir, tropical climate

HIGHLIGHTS

- A tropical reservoir in Colombia was monitored for 7 years during the pre-filling, filling and post-filling phases.
- The main contribution is the estimation of GHG in a tropical reservoir using a floating static chamber and the inverted funnel method.
- This is the first investigation carried out in Colombia to determine the net emissions in a reservoir.

GRAPHICAL ABSTRACT

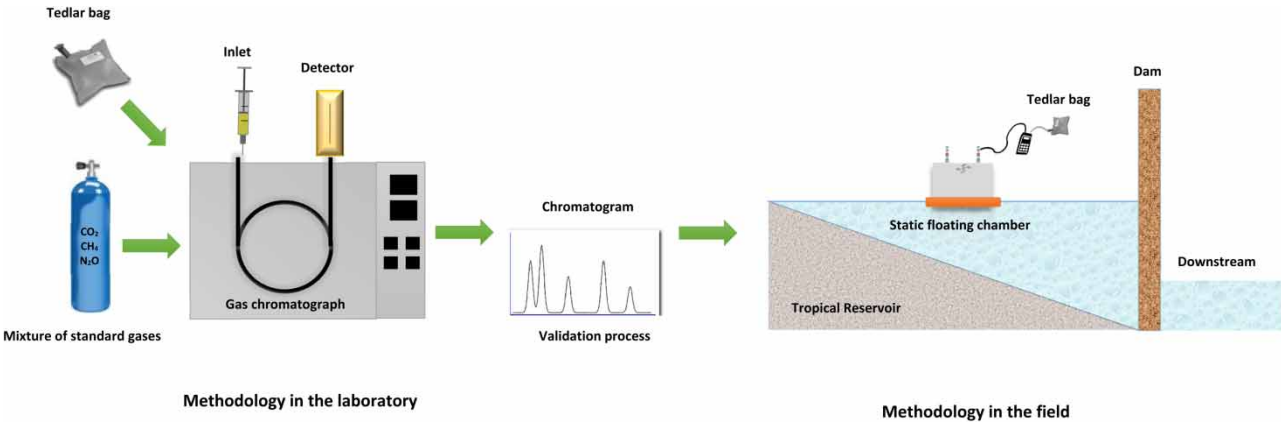

1. INTRODUCTION

Hydroelectric reservoirs are anthropogenic aquatic systems built over wide geographic extensions that are of great importance for energy production (Ometto *et al.* 2013; Barbosa *et al.* 2018). Traditionally, hydroelectric energy has been considered a form of clean energy (Abbasi *et al.* 2020); however, some have questioned this because the reservoirs release greenhouse gases (GHG) such as carbon dioxide and methane (Ometto *et al.* 2013; Burciaga *et al.* 2019), although these emissions are higher in the first years of operation of the reservoir. This was confirmed by Abril *et al.* (2005) and Teodoru *et al.* (2010), who observed in hydroelectric reservoirs that the vegetation and organic matter in the soil are transformed in the initial flood phase at high rates by bacterial activity, but after several years, GHG emissions significantly decrease (Teodoru *et al.* 2012), to the point that hydroelectric reservoirs emit less GHG than other energy sources, emitting 35–70 times less GHG than thermal power plants (Kumar & Sharma 2012).

In reservoirs, when organic matter is degraded by biological processes, GHG is generated. This organic matter is mainly made up of grasses, leaves and shrubs that contain lignocellulose, a polymeric material that hinders degradation processes, allowing organic matter to remain for years in the reservoir (Anvesh & Prasad 2016). The decomposition of organic plant matter during the first years after the filling is known as the maturation process of the reservoir and lasts for an average of 5–8 years, occurring with or without oxygen, depending on the conditions of the environment. This process can cause, at the beginning of the operation of the reservoir, significant emissions of carbon dioxide (CO_2) and methane (CH_4) (Lu *et al.* 2020).

GHGs are released through three processes: the diffusion process that takes place on the surface of the water; the bubbling that takes place at the bottom of the reservoir; and the degassing process in which the reservoir water is released through turbines and landfills when discharged through the dam. In this last phenomenon, the pressure on the water suddenly drops and, according to the chemical principle of Henry's Law, the capacity to retain dissolved gas is reduced, causing this to be released from the water through degassing emissions. These emissions are also due to the increased air/water interface that is created when water is sprayed at the bottom of a large landfill (Richey *et al.* 2002).

The carbon dioxide from both aerobic and anaerobic processes emitted from reservoirs for the generation of electrical energy has been estimated at 48Tg of CO_2 each year, which represents 9% of the total emissions from natural lakes (Barros *et al.* 2011). To determine the carbon balance of a reservoir, it is important to take into account several aspects in order to determine its real contribution to greenhouse gas (GHG) emissions. Thus, it is important to carry out measurements to quantify greenhouse gas emissions before the construction of the reservoir, since the net emissions produced by a hydroelectric project are determined by the difference between the emissions before and after this (Rocha *et al.* 2015). One aspect to consider from the pre-fill of the reservoir is the contribution of rivers, which naturally emit large amounts of CO_2 due to the decomposition of terrestrial organic matter (Mendonça *et al.* 2012).

The quantification of the net GHG emissions caused by a reservoir must consider the emissions before, during and after its construction. However, it must be taken into account that there are not only temporal but also spatial variations in GHG emissions associated with a reservoir, caused by factors including temperature, type and density of flooded vegetation and carbon loads. Greenhouse gas (GHG) emissions in reservoirs have been shown to be influenced by the climate with the lowest emissions in cold and temperate climates and, conversely, the highest in tropical areas (IHA 2010). In reservoirs, temperature, precipitation (Javadinejad *et al.* 2020), shape, depth, area, hydraulic retention time, age, type of ecosystem flooded, oxygenation system, entry of carbon (organic matter) and nutrients into the reservoir, primary productivity, and prevailing conditions in the basin such as erosion, deforestation and sanitary conditions, among other factors, affect the formation and emission of GHG (García *et al.* 2010; Obianyo 2019; Oo *et al.* 2020).

In Colombia, studies on reservoirs have mainly focused on evaluating water quality and limnology (Aguirre *et al.* 2007). The GHG estimation and quantification process has recently started. However, to date, no information has been reported on the net and gross emissions of these bodies of water before flooding that allows the percentage of these values to be established and compared with those reported for other activities in the national GHG inventory.

Greenhouse gas emissions were quantified in the pre-filling, filling and post-filling stages of a tropical reservoir located in the department of Santander in Colombia for 7 years, with the objective of evaluating the spatial and temporal variations of GHG emissions and to be able to define the impact associated with the generation of GHG from a reservoir in its initial stage of operation. This research is unique in Colombia since it managed to evaluate the impacts in different stages of filling a reservoir.

2. MATERIALS AND METHODS

2.1. Study area

The study was carried out in a reservoir located in Colombia, in the department of Santander (Figure 1), 75 km upstream from the mouth of the Magdalena river and 62 km downstream from the confluence of the Suárez and Chicamocha rivers. The average temperature of the area ranges from 24.6 to 32.0 °C in the day and 21.4 to 26.7 °C at night (IDEAM 2017), with slight increases in dry or transitional seasons. The average windspeed fluctuates between 0.1 and 0.3 m/s and the average humidity percentage is 51% (Ruiz *et al.* 2019). The reservoir uses the waters of the River Sogamoso in the generation of electricity through a 190 m high dam, a surface of water body of 6,960 ha, a total volume of 4,800 m^3 and an underground powerhouse with three generating units. With 820 MW of installed capacity and an average annual generation of 5,056 GWh-year, it is the hydroelectric plant with the four highest installed capacities in Colombia. In all sampling campaigns, data on temperature, precipitation, filling and height of the water sheet were taken into account in order to correlate the information obtained on greenhouse gas emissions. The height data were converted to area and volume using the reservoir bathymetry.

2.2. Greenhouse gas sampling campaigns

To assess the generation of GHG in the reservoir, time monitoring was performed during the pre-filling stage (in the tributaries) and the filling and post-filling stages in the reservoir (Table 1).

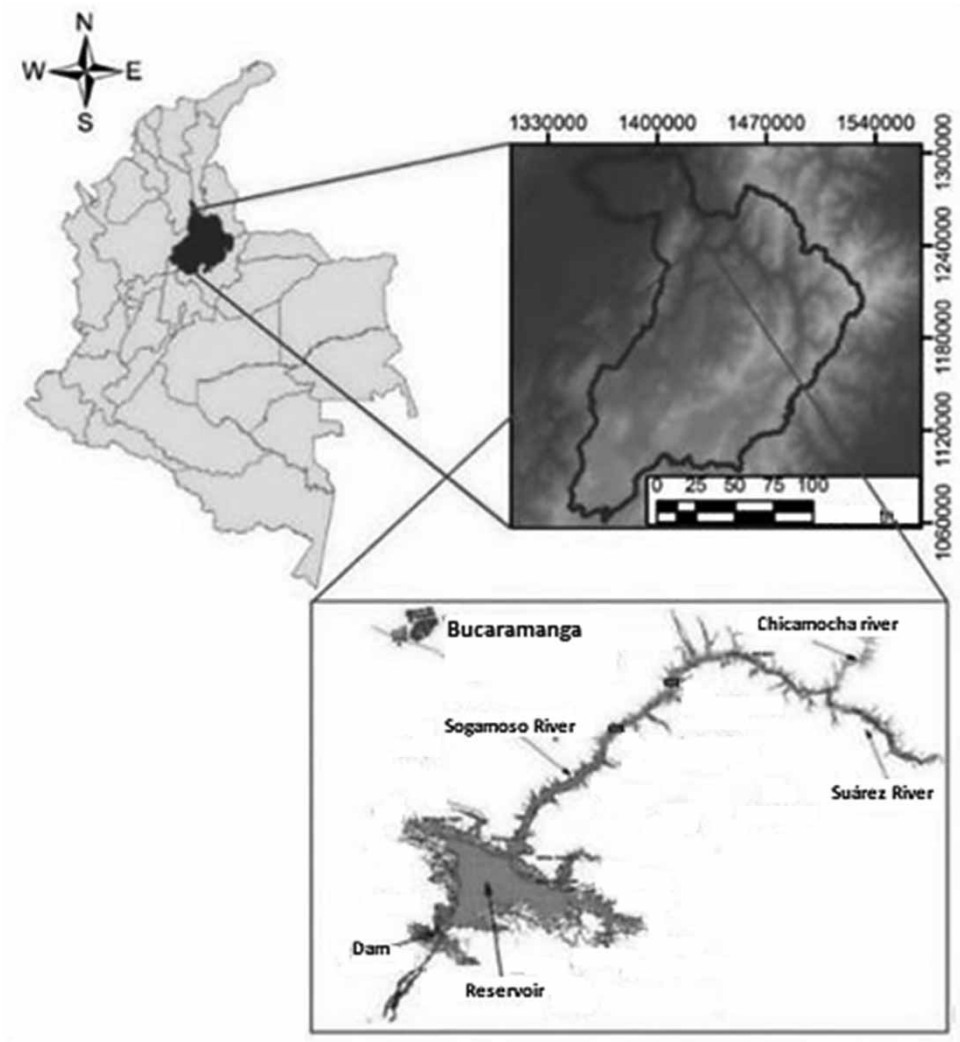

Figure 1 | Map of the study area (adapted from Lopera *et al.* 2016).

Table 1 | Distribution of monitoring from 2013 to 2019

Stage	N°	Month	Year	Season	Filling (%)
Pre-filling	Pre-sampling	March	2013	Dry	–
	M1	May		Rain	–
	M2	July		Dry	–
	M3	October		Transition	–
	M4	November		Rain	–
	M5	February	2014	Dry	–
Filling	M1	September	2014	Dry	25.0
	M2	November		Rain	59.5
	M3	November		Rain	83.4
Post-filling	M1	February	2015	Dry	66.0
	M2	May		Rain	60.5
	M3	September		Transition	59.0
	M4	November		Rain	71.0
	M5	March	2016	Dry	56.6
	M6	May		Rain	67.0
	M7	August		Dry	45.7
	M8	October		Rain	52.3
	M9	February	2017	Dry	73.6
	M10	June		Transition	98.5
	M11	September		Dry	71.0
	M12	November		Rain	96.7
	M13	March	2018	Dry	50.7
	M14	June		Rain	98.7
	M15	August		Dry	95.3
	M16	November		Rain	98.5
	M17	March	2019	Dry	65.8
	M18	June		Rain	94.6
	M19	September		Dry	88.6
	M20	October		Rain	91.3

2.2.1. Pre-filling of the reservoir

Before filling the reservoir, nine tributary rivers were selected upstream and one river downstream of the reservoir (Table 2), in order to establish the base line of GHG emissions. For the selection of the sampling points, the recommendations defined in the GHG measurement guidelines for freshwater reserves (IHA 2010) were taken into account.

Table 2 | Location of the sampling points in the pre-filling stage

N°	Sampling point	Description	Average flow (m^3/s)
1	R1	Downstream of the dam to 2.17 km	448.910
2	R2	Tributary	161.470
3	R3	Tributary	85.093
4	R4	Tributary; Confluence between R2 and R3	365.090
5	R5	Tributary	8.684
6	R6	Tributary	0.884
7	R7	River mouth tributary R6	0.884
8	R8	Tributary to 28 km from R4	365.090
9	R9	Tributary	0.926
10	R10	Tributary to 23 km from R4	365.090

Pre-sampling was carried out to adjust the dimensions of the GHG collection equipment (the UNESCO/IHA GHG Measurement Guidelines recommend the type and form of the equipment, but not the dimensions), and five samples were carried out for the GHG determination (Table 1). The samplings were scheduled taking into account the hydrological behavior in R4, the main tributary of the reservoir, in order to have sampling campaigns at different times of the year, according to the annual cycle of multi-year average flows.

2.2.2. Filling the reservoir

Measurements during the filling of the reservoir were carried out downstream and upstream of the tributary rivers and at two points located along the longitudinal axis of the reservoir. In total, four sampling points were selected (Table 3).

The filling evaluation phase was carried out during three sampling campaigns (Table 1), with the filling percentage of the reservoir being the selection criterion for each sample. The aim was to assess how the GHG generation of this body of water varied, taking into account the baseline established in the pre-fill and the characteristics of the tributaries that supply it.

2.2.3. Post-filling of the reservoir

Post-fill measurements were carried out at points located along the longitudinal axis through the reservoir and near the dam (Table 4). In total, eight sampling points were selected.

The post-filling evaluation was carried out during 20 sampling campaigns between the years 2015 and 2019 (Table 1). As in the pre-filling stage, the samplings were scheduled taking into account the hydrological behavior according to the annual cycle of multi-year average flows of the study area, in order to have sampling campaigns at different times of the year. Likewise, the filling percentage was established in each sampling, in the same way as during the filling of the reservoir. Additionally, nictemeral evaluation was carried out, in which gas samples were collected to evaluate the variation of day and night emissions, following the same methodology as for daytime sampling.

2.3. Determination of diffusive emissions

The diffusive fluxes of CO_2 and CH_4 were measured at the air–water interface at the different sampling points, using the floating static chamber method (Figure 2(a)) established by the IHA (2010). The acrylic chamber was designed by the GDCON research group, with dimensions of 0.4 m width × 0.4 m length × 0.5 m height, and a capacity to function at a depth of 0.3 m.

Table 3 | Location of sampling points during the filling stage

N°	Sampling point	Description	Average flow (m^3/s)
1	R1	Downstream of the dam	448.910 m^3/s
2	R4	Tributary	365.090 m^3/s
3	E3	Reservoir	–
4	E8	Reservoir	–

Table 4 | Location of sampling points in the post-filling stage

N°	Sampling point	Description[a]
1	E1	Dam
2	E2	4.3 km
3	E3	5.09 km
4	E4	9.74 km
5	E5	10.34 km
6	E6	11.54 km
7	E7	14.73 km
8	E8	16.02 km

[a]Distance from E1.

Figure 2 | Determination of emissions. (a) Floating static chamber. (b) Inverted funnel for bubble measurement.

The camera was submerged in the water and, by means of lateral floats, its stability was guaranteed and the movement due to the current was reduced. Two quick-closing valves were located in the upper part of the chamber; one as a purge valve to equalize the pressures before starting the measurement, and the other with a flexible hose that was connected to a gas collection pump, which extracted the gas from the acrylic box with a flow rate of 55 mL/min and stored it in Tedlar bags with a capacity of 0.5 L. The chamber had a fan inside, which allowed the air inside the chamber to be homogenized.

For the measurement of diffusive fluxes, four samples were taken at each point, every 7 min, for a total of 28 min of monitoring (IHA 2010; Sousa *et al.* 2019). This methodology was performed in order to provide data to perform linear regressions over time and to quantify the amount of both CO_2 and CH_4. The results were accepted or rejected following the methodology proposed by Lambert & Fréchette (2005). Finally, the correlation coefficient between the concentration of each gas versus time ($R^2 > 0.90$) and the analysis of variance ($p < 0.05$) were determined according to the methodologies proposed by Sousa *et al.* (2019), Guérin & Abril (2007) and Soumis *et al.* (2004). The diffusive fluxes in units of $g/m^2 \cdot d$ were determined from the ideal gases equation, using the following equation.

$$CO_2 \text{ or } CH_4 (g/m^2 \cdot d) = \frac{P \,.\, X \,.\, V_{FC} \,.\, W_1}{V_{TB} \,.\, R \,.\, T \,.\, A_{FC}} \quad (1)$$

where P is the atmospheric pressure (atm); X is the linear regression slope of the gas collected volume versus time (L/d); V_{FC} is the volume of the floating chamber (L); W_1 is the molecular weight of CO_2 or CH_4 depending on the calculation made (g/mol); V_{TB} is the volume of the tedlar bag (L); R is the universal gas constant (atm L/mol K); T is the temperature (K) and A_{FC} is the area of the floating chamber (m^2). For this study, a P of 0.895 atm, V_{FC} of 32 L, W_1 of 46 g CO_2/mol and 16 g CH_4/mol, V_{TB} of 0.5 L, R of 0.08206 atm L/mol K and A_{FC} of 0.16 m^2 were considered. In the case of T, the value changed according to weather conditions.

As an analytical control of the sampling, for points R1, R5, E1 and E8, samples were taken in duplicate, using two floating chambers of equal size, simultaneously. The samples were collected and taken to the GDCON group laboratory, where they were analyzed in a maximum time of 7 days, as suggested by Lambert & Fréchette (2005), using an Agilent 7890B gas chromatograph with a three-valve system and two detectors with packed 1/8' stainless steel columns (HayeSep Q 80/100), with 5975C mass detector for determination of both CO_2 and CH_4 (Hoyos *et al.* 2021).

2.4. Determination of emissions by bubbling

Bubble methane fluxes were estimated using the inverted funnel method (IHA 2010), with a specific design by the GDCON group. This device consisted of a 1 m diameter cone connected to a silicone hose, which in turn was connected at the upper end to a 0.5 L Tedlar bag in which the sample was collected and, at the lower end, assembled to a rigid rod that allowed the passage of gases. The cone had four weights distributed in its diameter, which allowed it to collect the sample at a depth of 4 m in the water column. Additionally, the system had a buoy that counteracted the weight, and allowed the funnel to float (Figure 2(b)).

The measurement was carried out for four uninterrupted hours, counted from the moment the equipment was placed in the water. After this, the samples were taken to the GDCON laboratory where they were analyzed in a maximum time of 7 days (Lambert & Fréchette 2005), using an Agilent 7890B gas chromatograph, with a 5975C mass detector.

The bubbling fluxes in units of g/m^2 d were determined from the ideal gases equation using the following equation:

$$CH_4(g/m^2d) = \frac{C \cdot X \cdot V_F \cdot W_1}{V_{TB} \cdot R \cdot T \cdot A_F} \quad (2)$$

where P is the atmospheric pressure (atm); C is the collected volume of the gas in a time of 4 h (L/d); V_F is the volume of the inverted funnel (L); W_1 is the molecular weight of CH_4 (g/mol); V_{TB} is the volume of the Tedlar bag (L); R is the universal gas constant (atm L/mol K); T is the temperature (K) and A_F is the area of the inverted funnel (m^2). For this study, a P of 0.895 atm, V_F of 68 L, W_1 of 16 g CH_4/mol, V_{TB} of 0.5 L, R of 0.08206 atm L/mol K and A_F of 2.54 m^2 were considered. In the case of T, the value changed according to weather conditions.

2.5. Statistical analysis

To observe the spatial and temporal variation of GHG emissions at the different points and during the different samplings, an exploratory analysis of the data, box and whisker plots, and a frequency histogram were performed. Additionally, the correlations between the studied variables were determined. Statistical analysis was performed using R software version 3.5.1.

3. ANALYSIS AND DISCUSSION

3.1. Emissions in pre-filling

Figure 3 shows the variation of CO_{2eq} in each sampling, taking into account that during the pre-filling, no CH_4 concentrations were detected in the diffusive fluxes. It is observed that both M2 and M5 presented similar average values (38,269.35 and 34,916.22-ton CO_{2eq}/year, respectively). These were both in the dry season and were the lowest values of all the five

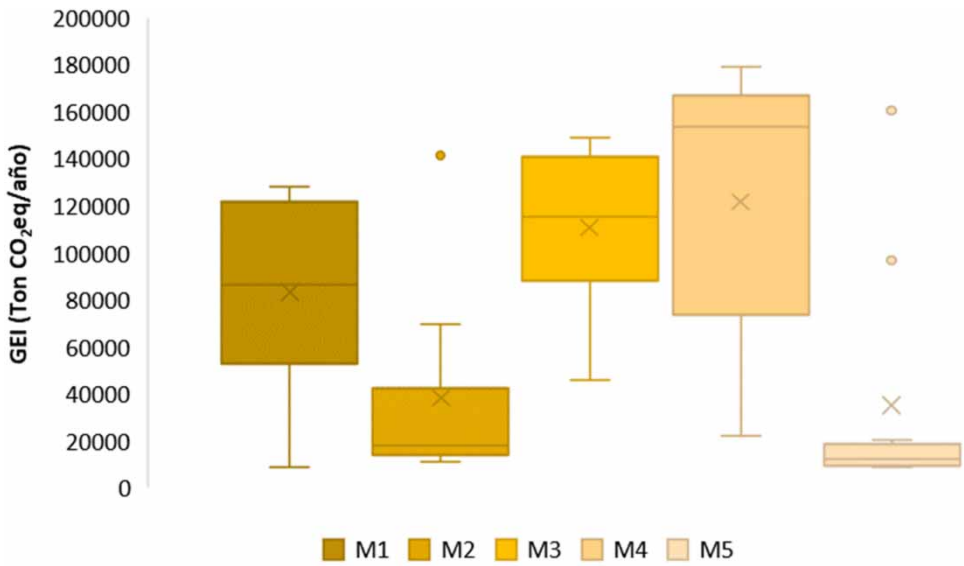

Figure 3 | Variation of CO_{2eq} during pre-fill sampling.

monitoring sessions carried out during the pre-fill. On the other hand, the highest fluxes were in rainy seasons and in transition (M1, M3 and M4), with averages of 83,084.32-ton CO_{2eq}/year in M1; 110,704.09-ton CO_{2eq}/year in M3 and 121,636.61-ton CO_{2eq}/year in M4. This trend was associated with mixing phenomena, which accelerate the degradation processes, allowing a greater transfer and in turn a greater diffusion of CO_2. In general, during the M4 sampling corresponding to the rainy season, the highest values in CO_2 emissions were presented, while for the M5 sampling corresponding to the dry season, low emissions were presented.

The multidimensional analysis that showed the Pearson product moment correlations between each pair of variables allowed us to statistically demonstrate the similarity between the pairs M1–M4 and M2–M5 ($p < 0.05$), that is, they were correlated with each other, M1–M4 being in the rainy season and M2–M5 in the dry season. In addition, in order to determine the means that were significantly different from each other, a multiple range contrast test was applied, finding an important difference in CO_{2eq} between the sampling pairs: M1–M2, M1–M5, M2–M3, M2–M4, M3–M5 and M4–M5, which demonstrates an influence of the time of year on the variation of CO_{2eq} emissions in rivers. It is important to highlight that the variability in rainfall can generate different seasonal patterns, modifying the circulation time of the water and producing variations in the intensity of the environmental processes that occur in aquatic systems. On the other hand, the external load of organic matter and other compounds in the system increases with episodes of intense rainfall (Armengol *et al.* 1999), due to the associated runoff. Additionally, precipitation affects CO_2 transfer, causing turbulence and thus inducing CO_2 flow through the air–water interface (Takagaki & Komori 2007).

With respect to each sampling point (Figure 4), R6 presented, on average, the highest CO_2 flow of all the points (8.050 g CO_2/m^2 d) at the pre-filling stage. This was associated with the proximity of R6 to cattle grazing areas, which increases the concentrations of organic matter, and therefore CO_2. On the contrary, R8 was the station with the lowest emissions (2.019 g CO_2/m^2 d), while R4, R5 and R10 presented the greatest variability in data. Of these sites, R4 and R10 are in areas of high mining exploitation, and R5 corresponds to the main river of a municipality, to which domestic wastewater discharges are discharged. For the stations R1, R7 and R9, some atypical data were presented, which is to be expected due to the variability of the weather periods of each sampling.

The data found for the 10 rivers in this study were found in a range of 2.048 to 8.050 g CO_2/m^2 d. When comparing these results with studies carried out by other authors (Table 5), a high variation is found in the information, particularly for tropical climates, where authors such as Guérin *et al.* (2006) found CO_2 values of the order of 37.796 g CO_2/m^2 d, while Richey *et al.* (2002) reported an average of 8.316 g CO_2/m^2 d, the latter value being much more in line with what was found in this study. Other investigations carried out in rivers in boreal climates have reported values in the range of 0.36 g CO_2/m^2 d (Wang *et al.*

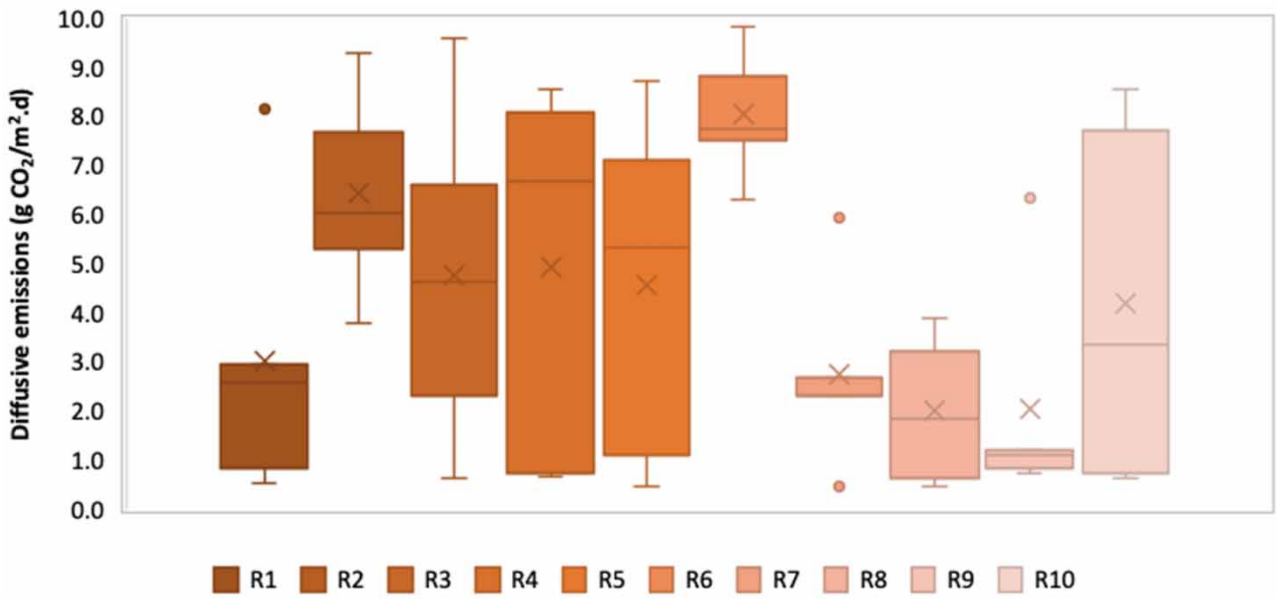

Figure 4 | CO_2 diffusive flux emissions in the tributaries of the reservoir in the pre-filling stage.

Table 5 | Comparison of CO_2 emissions in rivers with other studies

River	Country	g CO_2/m^2 d	References
Mekong River	China	8.559	Li *et al.* (2013)
Xiangxi River		0.384	Huang *et al.* (2014)
Maotiao River		0.36–2.8	Wang *et al.* (2010)
Yellow River		23.221	Qu *et al.* (2017)
River in Ontaro	Canada	3.960	Koprivnjak *et al.* (2010)
River in Quebec		11.444	Teodoru *et al.* (2009)
Mississippi River	United States	11.884	Dubois *et al.* (2010)
River	Sweden	30.356	Humborg *et al.* (2010)
Amazonian rivers	Brazil	8.316	Richey *et al.* (2002)
Tropical rivers		37.796 ± 17.600	Guérin *et al.* (2006)
R1	Colombia	3.020 ± 2.062	In this study
R2		6.432 ± 2.138	
R3		4.762 ± 3.524	
R4		4.951 ± 2.940	
R5		4.557 ± 3.644	
R6		8.050 ± 1.338	
R7		2.745 ± 1.986	
R8		2.019 ± 1.528	
R9		2.048 ± 2.402	
R10		4.210 ± 2.769	

2010) to 30.356 g CO_2/m^2 d (Humborg *et al.* 2010), which shows that, in the case of rivers, gas emissions may be more associated with the presence of organic matter or with land uses near the areas of influence of the rivers than with the associated climate regime.

3.2. Emissions in the filling stage

Table 6 shows the CO_2 fluxes emitted for each of the filling percentages of the monitored reservoir. In this case, no diffusive fluxes of CH_4 were found, that is, during this stage, strictly anaerobic conditions were not established at the bottom of the reservoir, which would give rise to emissions of this gas.

Points R1 and R4 correspond to rivers downstream and upstream of the reservoir, respectively. For point R1, the CO_2 emissions in the three samplings were very similar, indicating that the filling percentage of the reservoir had no impact on the generation of CO_2 at this point. This was to be expected at this stage, in which there was not yet energy generation that could give rise to the degassing phenomenon, which tends to increase gases downstream from the dam. On the other

Table 6 | CO_2 fluxes at monitored points during filling of the reservoir

	(g $CO_2/m^2 \cdot$ d)			
	Filling percentage			
Sampling point	25.00%	59.50%	83.40%	Average
R1	1.019	1.205	1.300	1.175
R4	2.724	4.024	4.690	3.813
E3	5.564	9.991	9.195	8.250
E8	6.188	10.696	15.533	10.806

hand, comparing the range of CO_2 emitted at point R1 during the pre-filling (0.555–8.163 g CO_2/m^2 d) with the range in the filling (1.019–1.300 g CO_2/m^2 d), we find that the values are within the same order of magnitude; therefore, there is no significant difference. Regarding point R4, located at the tail of the reservoir, a slight increase in CO_2 emissions was evidenced with the filling percentage of the reservoir, with a minimum value of 2.724 g CO_2/m^2 d and a maximum of 4.690 g CO_2/m^2 d for filling percentages of 25.00 and 83.40%, respectively. This is due to the increase in the water column over the plant material, which accelerates the degradation processes of organic matter and gives rise to the release of more CO_2.

During filling, the maximum average value of CO_2 emissions was at point E8 in the reservoir (10.806 g CO_2/m^2 d), and the minimum was found at point R1 (1.175 g CO_2/m^2 d). For all points, the highest emission values were reported for the highest filling percentage of the reservoir (83.40%), with 1.300 g CO_2/m^2 d for point R1, 4.690 g CO_2/m^2 d for R4, 9.195 g CO_2/m^2 d for E3 and 15.533 g CO_2/m^2 d for R8. The minimum CO_2 emission values were reported for the lowest percentage of reservoir filling (25.00%) in each of the points, indicating that the higher the water volume, the more flooded area and, therefore, the more decomposing vegetation generating more CO_2. This is confirmed by the statistical analysis that showed a correlation between the filling percentage and CO_2 emissions ($p < 0.05$). At this stage, it was not possible to correlate the climatic variation with the CO_2 emissions, since the filling of the reservoir was carried out in 3 months, so a high seasonal variation did not occur between each sampling.

The point that presented the highest emissions in the reservoir during the three samplings carried out was station E8. This point is influenced by the discharge of organic matter from the R5 river, which is the recipient of wastewater from a nearby municipality, so the increase in CO_2 emissions is due not only to the decomposition of the flooded organic matter but also to the contribution of organic matter that enters through the R5 river. Another factor that probably had an impact on the generation of gases between one point and another in the reservoir is the use that the soil had before the flood since there were areas where there had been intensive use of livestock, which generates a greater contribution of organic matter in the area, thus increasing GHG production.

Comparing the results obtained from the CO_2 fluxes at points E3 and E8 of the reservoir, with the data reported in the literature, it is found that UNESCO/IHA (2008) and Integrated Environments (2006) report average diffusive fluxes of 9.086 g CO_2/m^2 d in reservoirs with a tropical climate, with minimum values of 0.836 g CO_2/m^2 d and maximum values of 19.008 g CO_2/m^2 d. This suggests that the data found for this study (on average 8.250 g CO_2/m^2 d for E3 and 10.806 g CO_2/m^2 d for E8) are within this range.

3.3. CO_2 emissions in post-filling stage

Figure 5 shows the results of both diffusive and bubbling fluxes during post-filling. The highest CO_2 emissions occurred at points E1 and E8, with average values of 20.508 and 22.405 g $CO_2/m^2 \cdot d$, respectively (Figure 5(a)). E1 is the point in the dam where the gases begin to accumulate until they are finally released by the degassing process. E8 is the furthest point from the reservoir, at the point of discharge of the R5 river which, as previously mentioned, crosses a municipality where discharges of domestic wastewater occur. With regard to the lowest CO_2 emission, station E3 obtained an average value of 16.843 g $CO_2/m^2 \cdot d$, this point being on the longitudinal axis of the reservoir. Comparing these results with the literature, it is found that the values in this study are slightly higher than those reported by UNESCO/IHA (2008) and Integrated Environments (2006) for diffusive fluxes in tropical reservoirs, which show an average of 9.086 g $CO_2/m^2 \cdot d$ with a minimum of 0.836 g $CO_2/m^2 \cdot d$ and a maximum of 19.008 g $CO_2/m^2 \cdot d$. In this case, it is important to highlight that the age of the reservoir plays a fundamental role in GHGs, since very young reservoirs, like the one in this study, tend to have higher emissions due to the degradation process of flooded organic matter which, over time, tend to decrease or stabilize. This phenomenon has been reported by authors such as Valle & Kaplan (2019) and Campo & Sancholuz (1998), who found that the decomposition of easily degradable organic matter occurred over a period of 10 years, after which time decomposition was slower, with a loss of 43% of totally flooded organic matter after 37 years.

Meanwhile, regarding methane emissions, Figure 5(b) shows the variation of diffusive fluxes. In this case, as with the CO_2 flow, the maximum value was presented in E8 (0.455 g $CH_4/m^2 \cdot d$) and the minimum in E2 (0.037 g $CH_4/m^2 \cdot d$), located on the transverse axis of the reservoir. These results are of the same order of magnitude as reported by UNESCO/IHA (2008) and Integrated Environments (2006) with an average of 0.410 g $CH_4/m^2 \cdot d$ and a minimum and maximum of 0.0048 and 0.816 g $CH_4/m^2 \cdot d$, respectively. Comparing these results with studies of other reservoirs, both tropical and boreal (Table 7), it is found that the maximum value in this study is much higher than those reported elsewhere, with the exception of the Balbina reservoir, where a value of 1.128 g $CH_4/m^2 \cdot d$ was reported. Finally, CH_4 emissions by bubbling (Figure 5(c))

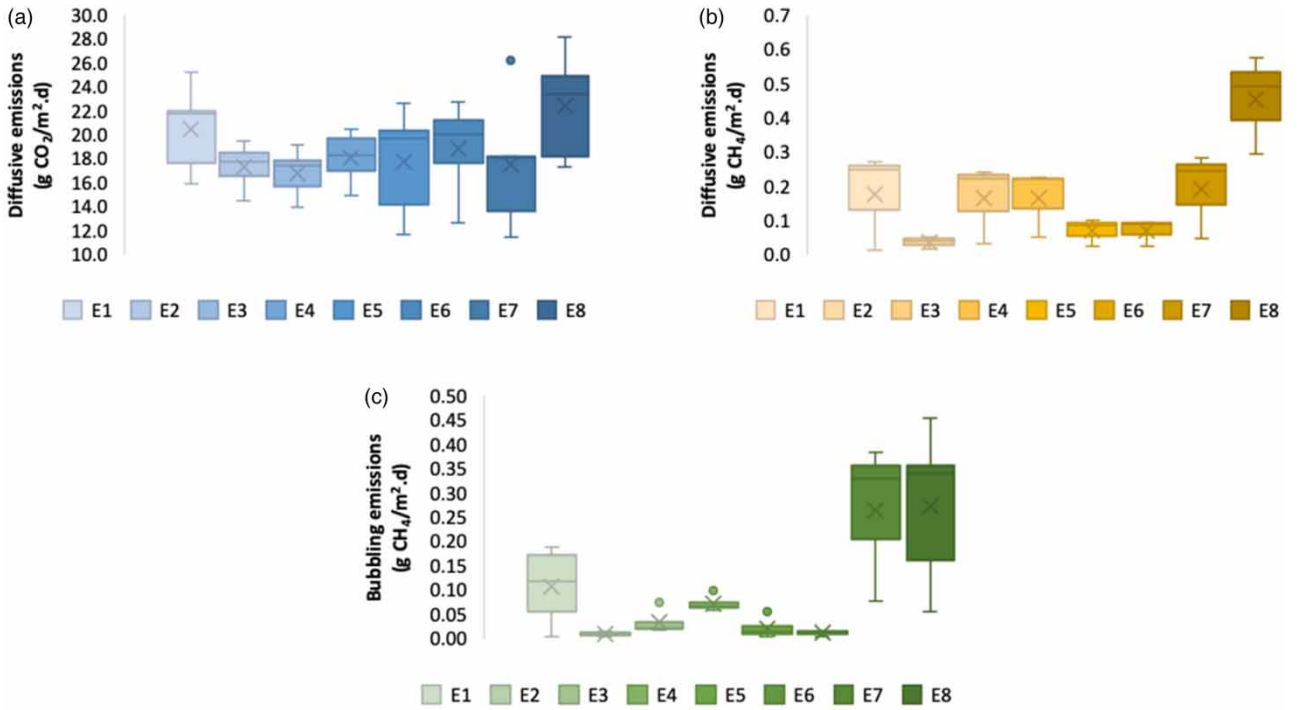

Figure 5 | Analysis of diffusive and bubbling fluxes in the post-filling stage. (a) Diffusive CO_2 emissions. (b) CH_4 diffusive emissions. (c) CH_4 bubbling emissions.

were higher at points E1, E7 and E8, with values of 0.107, 0.264 and 0.274 g $CH_4/m^2 \cdot d$, respectively. These correspond to the point of the dam (E1) and the furthest points in the longitudinal axis of the reservoir (E7 and E8), where in addition to the contribution of organic matter that reaches them through the rivers, there are also laminar flow conditions, with few intrusive currents and a prevalence of advective phenomena, which favors anaerobic conditions.

Regarding the generation of GHG from the reservoir according to the level of filling (Figure 6), it was found that there is a linear relationship ($p < 0.05$) with a correlation coefficient (R^2) of 0.8343. Therefore, it can be inferred that the higher the filling level of the reservoir, the greater the emissions generated by the system. This is also correlated with the weather season, since the highest filling percentages occurred in the rainy and transition season, with an average of 81.56%, and

Table 7 | CO_2 fluxes at monitored points during filling of the reservoir

Reservoir	Country	Diffusive g $CH_4/m^2 \cdot d$	Bubble	References
Petit Saut	France	0.014	0.0046	Abril *et al.* (2005)
Koomboolonba	Australia	0.229	–	Demarty & Bastien (2011)
Gatun	Panama	0.298	15.864	Keller & Stallard (1994)
Tres Marias	Brazil	0.032	0.164	Rosa *et al.* (1996)
Barra Bonita		0.017	0.924	
Tucurui		0.101	0.008	
Samuel		0.088	0.017	
Balbina		1.128	–	Kemenes *et al.* (2007)
Tropical Reservoirs	–	0.410 0.0048–0.816	0.705 0.000–1.408	UNESCO/IHA (2008) Integrated Environments (2006)
Reservoir	Colombia	0.037–0.455	0.010–0.274	In this study

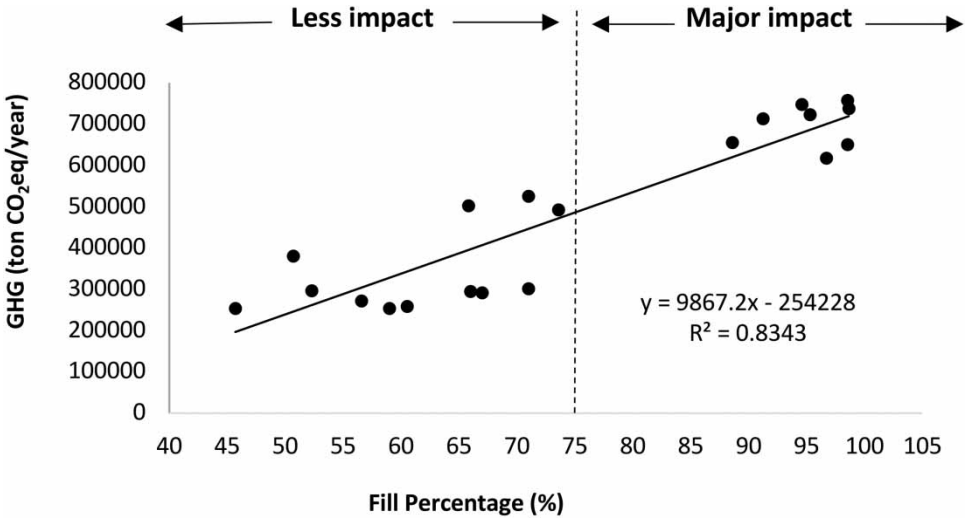

Figure 6 | Relationship between the filling percentage of the reservoir and GHG emissions.

the lowest (60.33% average) in the dry season. Likewise, the water level in the reservoir is a determining variable in the GHG emission processes, and it is recommended that the filling percentage of the reservoir should remain below 75% in order to minimize gas generation.

In any type of reservoir, during the first years after filling, GHG emissions tend to increase due to the rapid decomposition of flooded organic matter, mainly plant material. In this study, emissions increased from 2015 to 2019 (Figure 7), but these increases were less in 2015 and 2016, compared to 2017 to 2019. This indicates that, during the first two years of operation of the reservoir, the decomposition process of the plant biomass was slow, which is associated with the breaking of the polymer chains present in the plant material. According to García *et al.* (2010), the plant material has heterogeneous chemical compounds that include structural polymers of the cell wall (proteins, cellulose, hemicellulose and lignin) and soluble materials (simple sugars, amino acids, oils, waxes and phenols). Therefore, much of the organic matter present in plant biomass has high molecular weights. Organic matter of this nature generally has a first stage of microbial decomposition, called enzymatic hydrolysis, which occurs before biodegradation to low-intermediate organic metabolites of low molecular weight begins. These metabolites then produce CO_2–CH_4 (anaerobic processes) or CO_2 (aerobic processes). In 2015 and 2016, intermediate metabolites could have been formed, so the increase in emissions from 2017 to 2019 could be due to the decomposition of low molecular weight metabolites, such as amino acids and disaccharides, that can degrade faster.

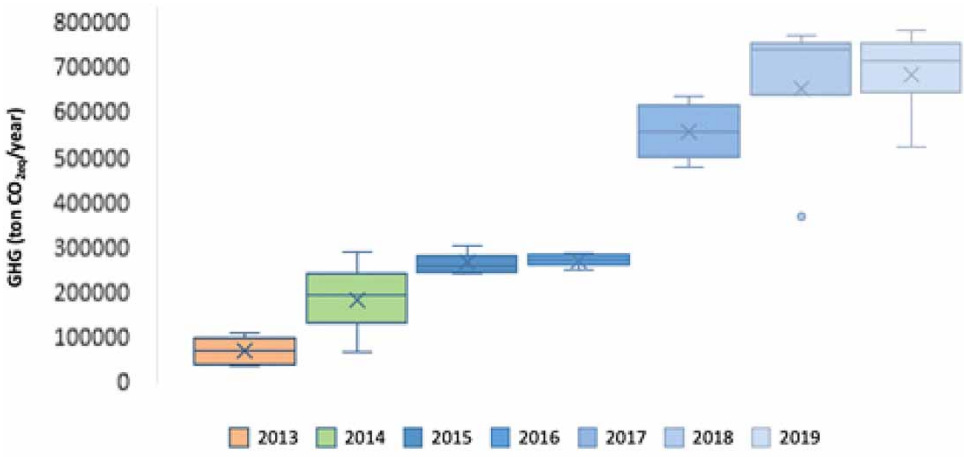

Figure 7 | Comparison of CO_{2eq} in the pre-fill and post-fill stages of the reservoir.

Table 8 | CO_{2eq} emissions in the pre-filling, filling and post-filling stages of the reservoir

	Year	Gross emissions (ton CO_{2eq}/year)	Net emissions (ton CO_{2eq}/year)
Pre-filling	2013	70,892.51 ± 41,079.16	–
Filling	2014	178,254.53 ± 105,838.01	107,362.02
Post-filling	2015	256,613.70 ± 27,101.27	185,721.19
	2016	261,542.39 ± 16,246.99	190,649.89
	2017	534,863.07 ± 73,392.00	463,970.57
	2018	627,070.94 ± 182,665.94	556,178.43
	2019	654,642.72 ± 108,940.66	583,750.21

On the other hand, comparing the baseline (pre-fill) with the post-fill (Table 8), it is found that the CO_{2eq} emissions in the pre-fill stage were of the order of 70,892.51-ton CO_{2eq}/year, and in the post-fill stage 278,111.43-ton CO_{2eq}/year on average. This shows the incidence of flooded plant material and organic matter present in the water body, which contribute to the formation of GHG. It is important to highlight that the deviation of the data is relatively high, considering that different sources were monitored in the pre-filling stage, which contained variable concentrations of organic matter, total solids and nutrients, factors that affect microbial dynamics and in turn accelerate or decrease the gas emission process. In addition, all the monitoring was carried out in different climatic regimes, which has an impact on the rate of degradation of organic matter and on the transfer of gases in the air-water interface.

Taking stock of the emissions in the pre-fill (baseline) and the post-fill stages during the years 2015 to 2019 (Table 8), average net emissions were established in the post-fill stage of 396,054.058-ton CO_{2eq}/year. Considering that in the pre-fill stage this figure was 70,892.510-ton CO_{2eq}/year, there was an increase in gas emissions over the years in the reservoir due to the degradation of the flooded plant biomass and the organic load present in the tributary rivers.

To evaluate the mitigation potential of the buffer zone with respect to GHG emissions from the reservoir in 2019 (Table 9), the carbon balance of the system was calculated. On the one hand, the emissions of the reservoir correspond to the average emission of the reservoir in 2019 (654,642.72-ton CO_2eq/year) minus the emissions of bodies of water in the pre-filling (year 2013; 70,892.59-ton CO_2eq/year). While the mitigation potential of the buffer zone by aerial biomass corresponds to the amount of CO_2eq captured by aerial biomass (137,101.26-ton CO_2eq/year) minus soil emissions (19,680.33-ton CO_2eq/year) in 2019. In this way, the balance is 466,328.28-ton CO_2eq/year, which indicates that the protection band counteracts approximately 20% of the emissions produced in the reservoir.

Studies carried out by various authors have shown the high variability of CO_{2eq} emissions in tropical reservoirs (Figure 8), where factors such as the area and age of the reservoir constitute an additional variable in the process. Authors such as dos Santos *et al.* (2017), Demarty & Bastien (2011), Kemenes *et al.* (2007) and Rosa *et al.* (1996) carried out the analysis of nine tropical reservoirs with areas from 60 to 2,360 km^2 and ages from 1 to 36 years located in Brazil and reported GHG emissions of the order of 87,000.00-ton CO_{2eq}/year for the Segredo reservoir – 2,433,000.00-ton CO_{2eq}/year for the Balbina reservoir. On the other hand, in the case of Colombia, where there are no reports of measurements in the reservoir, authors such as Cuadros *et al.* (2019) applied a model to predict emissions in 12 reservoirs with areas from 3.4 to 150 km^2 and ages between

Table 9 | Carbon balance in the system in 2019

Description	t CO_{2eq}/año
Reservoir emission	654,642.72
Emission on pre-fill	70,892.59
Reservoir emission	**583,750.21**
Capture buffer zone (Aerial biomass)	137,101.26
Soil emissions	19,680.33
Capture buffer zone	**117,420.93**
Carbon balance	**466,328.28**

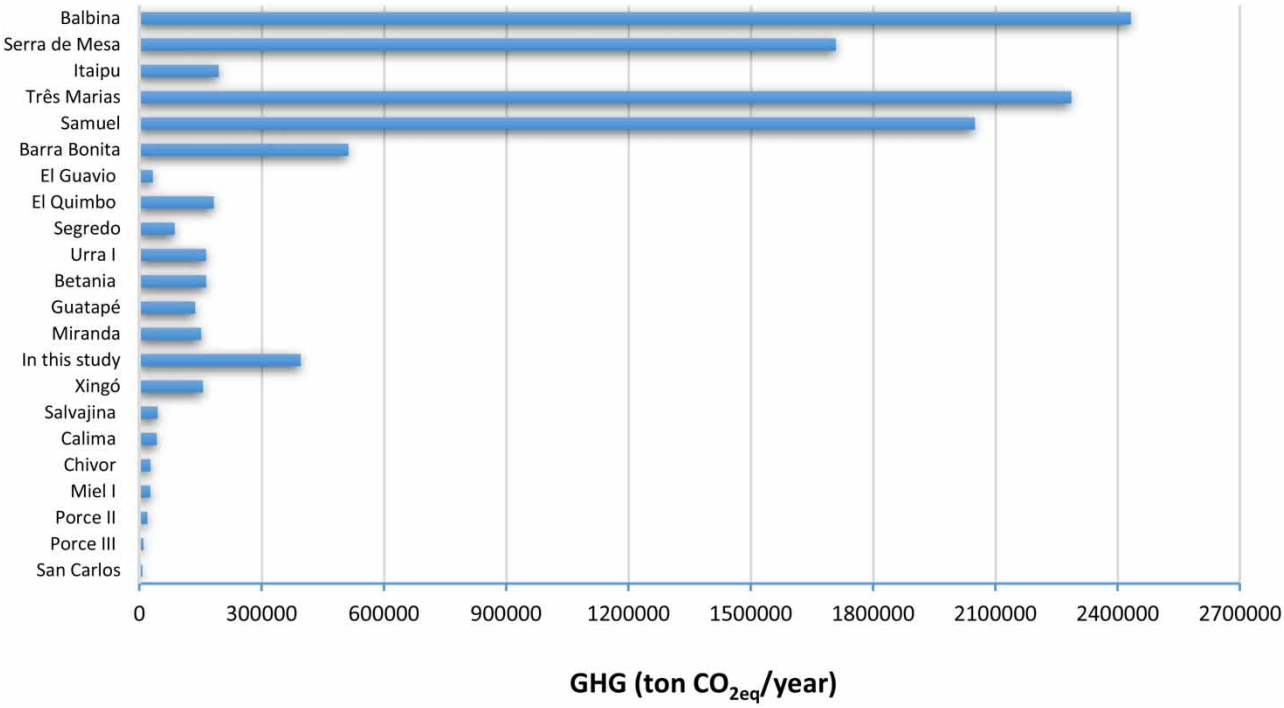

Figure 8 | GHG emissions reported in the literature in tropical reservoirs compared to this study. Reservoir area; San Carlos (3.4 km^2), Porce III (4.6 km^2), Porce II (8.9 km^2), Miel I (12.2 km^2), Chivor (12.6 km^2), Salvajina (31.0 km^2), Xingó (60.0 km^2), In this study (63.7 km^2), Miranda (70.0 km^2), Guatapé (74.0 km^2), Betania (74.0 km^2), Urra I (77.0 km^2), Segredo (82.0 km^2), El Quimbo (82.5 km^2), El Guavio (150.0 km^2), Barra Bonita (334.3 km^2), Samuel (560.0 km^2), Três Marias (1,155.0 km^2), Itaipu (1,350.0 km^2), Serra de Mesa (1,784.0 km^2), Balbina (2,360.0 km^2).

5 and 45 years, from data on diffusive emissions reported by the IPCC in 2006, where they estimated values in the range of 7,600.00-ton CO_{2eq}/year for the San Carlos reservoir – 182,700.00-ton CO_{2eq}/year for the Quimbo reservoir, values well below those found in the reservoir of this study. The tropical reservoir of this study, with average emissions of 396,054.058-ton CO_{2eq}/year, is within the values reported in the literature (Figure 8). However, compared to other reservoirs with similar areas, the reservoir in this study has higher emissions. This is attributable to the fact that this reservoir is relatively new, so the plant matter is in a high state of degradation. It would be expected that, with increasing age, emissions from the reservoir will decrease in line with the same reduction in the organic matter content and with respect to the other reservoirs

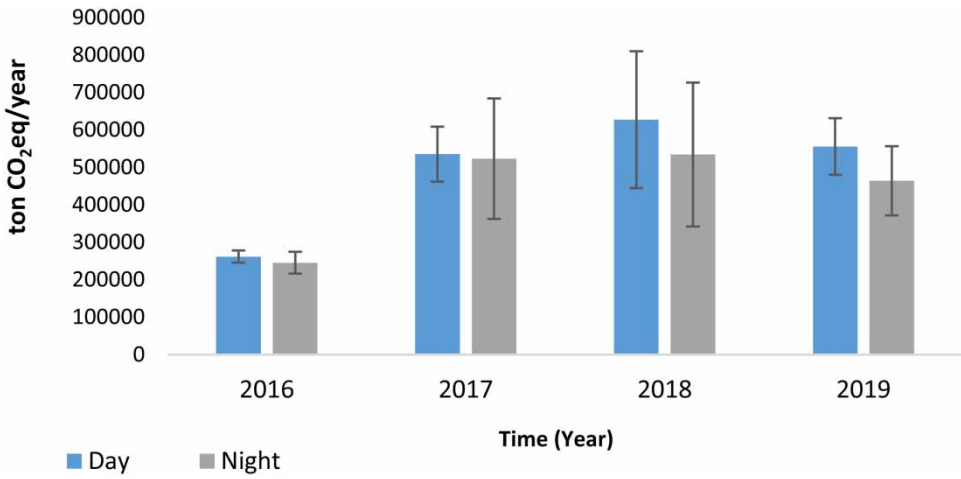

Figure 9 | Annual variation of GHGs during the day and night.

in Colombia, it is important to highlight that in the study of Cuadros *et al.* (2019) only the diffusive emissions were taken into account, without including those of bubbling and, furthermore, they constitute purely theoretical results.

Finally, comparing the day and night samples, it is concluded that gas emissions are greater during the day than at night, a situation that occurred in the samples of the years 2016, 2017, 2018 and 2019 (Figure 9). Herrera *et al.* (2013) found variations around 21–52% in gas emissions between day and night in a tropical reservoir, with those in the day being greater than those at night, and the highest emissions being specifically at 12 pm. They associated this situation with the difference between day and night temperatures since lower temperatures affected the metabolism of the microorganisms and therefore slowed down the degradation process. In this regard, in the case of this reservoir, the differences in day and night emissions were in the order of 6.3, 2.2, 14.8 and 16.4% for the years 2016, 2017, 2018 and 2019, respectively, percentages that are in the ranges found by Herrera *et al.* (2013). Additionally, in the study area, the average temperatures in the day range from 24.6 to 32.0 °C and at night between 21.4 and 26.7 °C (IDEAM 2017), which indicates that the temperature has a direct incidence on these processes.

4. CONCLUSIONS

This study represents the first greenhouse gas inventory available in a reservoir in Colombia, from the beginning of its operation to its start-up, and will serve as a contribution to future research in a country where the energy transition to other renewable sources is at the study stage. According to the results, in the reservoir, there was a high spatial variability in GHG emissions, which was mainly related to the presence of organic matter at the sampled points of the reservoir, that is, this spatial variation is influenced by the location of each sampling point and the tributaries that reach the reservoir. There is also temporal variability in the emissions, which is related to the level of the reservoir's water column (area, volume and percentage of filling, according to the bathymetry of the reservoir), which favors processes that enable CO_2 emissions. However, it was possible to demonstrate that the registered emissions are in the ranges established for tropical climates. The fact that the results obtained did not present a constant trend could be related to what was recorded in the bibliographic review, whereby in the first years of the reservoir, emissions tend to increase and be more significant, before stabilizing in later years. However, to verify what is described in the literature regarding CO_2 emissions during the first years after filling the reservoir, it is necessary to continue taking measurements for a longer period of time, enabling the respective comparisons with other studies and the creation of predictive models of CO_2 fluxes in the reservoir.

ACKNOWLEDGEMENTS

The authors gratefully acknowledge the financial support provided by the Colombian Scientific Program within the framework of the Ecosistema Cientifico call for proposals (Contract No. FP44842-218-2018). In addition, they thank the company ISAGEN and the GDCON group at the University of Antioquia for financing the work, through the agreement 47/26: 'Quantifying GHG emissions for the Sogamoso Hydroelectric Project'.

DATA AVAILABILITY STATEMENT

All relevant data are included in the paper or its Supplementary Information.

REFERENCES

Abbasi, T., Abbasi, T., Luithui, C. & Abbasi, S. A. 2020 A model to forecast methane emissions from tropical and subtropical reservoirs on the basis of artificial neural networks. *Water* **12** (145), 2–8. https://doi.org/10.3390/w12010145.

Abril, G., Guerin, F., Richard, S., Delmas, R., Galy-Lacaux, C., Gosse, P., Tremblay, A., Varfalvy, L., dos Santos, M. A. & Matvienko, B. 2005 Carbon dioxide and methane emissions and the carbon budget of a 10-year-old tropical reservoir (Petit-Saut, French Guiana). *Global Biogeochemical Cycles* **19**, GB4007. https://doi.org/10.1029/2005gb002457.

Aguirre, N., Palacio, J. & Ramírez, J. J. 2007 Características limnológicas del embalse El Peñol – Guatapé Colombia. *Revista de Ingeniería Univesidad de Medellín* **6** (10), 53–66.

Anvesh, G. & Prasad, C. 2016 Greenhouse gas diffusive flux assessment from few Indian reservoirs. *International Journal of Scientific & Engineering Research* **7** (7), 1–5. https://doi.org/10.4172/2157-7625.1000201.

Armengol, J., García, J. C., Comerma, M., Romero, M., Dolz, J., Roura, M., Han, B. H., Vidal, A. & Simek, K. 1999 Longitudinal processes in canyon type reservoirs: the case of Sau (N. E. Spain). In: *Theoretical Reservoir Ecology and its Applications* (Tundisi, J. G. & Straškraba, M., eds.). International Institute of Ecology. Brazilian Academy of Sciences and Backhuys Publishers, Leiden, pp. 313–345.

Barbosa, P. M., Farjalla, V. F., Melack, J. M., Amaral, J., da Silva, J. & Forsberg, B. 2018 High rates of methane oxidation in an Amazon floodplain lake. *Biogeochemistry* **137**, 351–365. https://doi.org/10.1007/s10533-018-0425-2.

Barros, N., Cole, J., Tranvik, L., Prairie, Y., Bastviken, D. & Huszar, V. 2011 Carbon emission from hydroelectric reservoirs linked to reservoir age and latitude. *Nature Geoscience* **4** (9), 593–596. https://doi.org/10.1038/ngeo1211.

Burciaga, U., Sáez, P. & Hernández, F. 2019 Strategies to reduce CO_2 emissions in housing building by means of CDW. *Emerging Science Journal* **3** (5), 274–284.

Campo, J. & Sancholuz, L. 1998 Biogeochemical impacts of submerging forests through large dams in the Rio Negro, Uruguay. *Journal of Environmental Management* **54**, 59–66. https://doi.org/10.1006/jema.1998.0222.

Cuadros, H., Cuellar, Y., Chiriví, J. S. & Guevara, M. 2019 GHG diffuse emissions estimation, and energy security to ENSO using MERRA-2 for largely hydroelectricity-based system. *Revista Facultad de Ingeniería* **91**, 70–82. https://doi.org/10.17533/10.17533/udea.redin.n91a07.

Demarty, M. & Bastien, J. 2011 GHG emissions from hydroelectric reservoirs in tropical and equatorial regions: review of 20 years of CH_4 emission measurements. *Energy Policy* **39**, 4197–4206. https://doi.org/10.1016/j.enpol.2011.04.033.

dos Santos, M. A., Machado, J., Pereira, J., Andrade, M., Mollica, A., Lucas, J., Pineiro, M. E., Cordeiro, A. & Pinguelli, L. 2017 Estimates of GHG emissions by hydroelectric reservoirs: the Brazilian case. *Energy* **133**, 99–107. https://doi.org/10.1016/j.energy.2017.05.082.

Dubois, K. D., Lee, D. & Veizer, J. 2010 Isotopic constraints on alkalinity, dissolved organic carbon, and atmospheric carbon dioxide fluxes in the Mississippi River. *Journal of Geophysical Research: Biogeosciences* **115**, 1–11. https://doi.org/10.1029/2009jg001102.

García, L., Rios, A. & Molina, L. 2010 Structure, plant composition and leaf litter decomposition in soil, at two sites of an Andean cloud forest (reforested and in spontaneous succession), in Peñas Blancas, Calarcá (Quindío), Colombia. *Actualidades Biológicas* **32** (93), 147–164.

Guérin, F. & Abril, G. 2007 Significance of pelagic aerobic methane oxidation in the methane and carbon budget of a tropical reservoir. *Journal of Geophysical Research: Biogeosciences* **112**, 1–14. https://doi.org/10.1029/2006jg000393.

Guérin, F., Abril, G., Richard, S., Burban, B., Reynouard, C., Seyler, P. & Delmas, R. 2006 Methane and carbon dioxide emissions from tropical reservoirs: significance of downstream rivers. *Geophysical Research Letters* **33** (21), 1–6. doi:10.1029/2006GL027929.

Herrera, J., Rojas, J., Rodríguez, S., Rojas, A. & Beita, V. 2013 Determinación de emisiones de metano en tres embalses hidroeléctricos en Costa Rica. *Revista de Ciencias Ambientales* **46** (1), 27–36. https://doi.org/10.15359/rca.46-2.3.

Hoyos, D., Gallego, S., Rodríguez, D. C. & Peñuela, G. A. 2021 Implementation of an analytical method for the simultaneous determination of greenhouse gases in a reservoir using FID/μECD gas chromatography. *International Journal of Environmental Analytical Chemistry* doi:10.1080/03067319.2021.1900148.

Huang, W., Bi, Y., Hu, Z., Zhu, K., Zhao, W. & Yuan, X. 2014 Spatio-temporal variations of GHG emissions from surface water of Xiangxi River in Three Gorges Reservoir region, China. *Ecological Engineering* **83**, 28–32. https://doi.org/10.1016/j.ecoleng.2015.04.088.

Humborg, C., Magnus, C., Sundbom, M., Borg, H., Bleckner, T., Giesler, R. & Ittekkot, V. 2010 CO2 supersaturation along the aquatic conduit in Swedish watersheds as constrained by terrestrial respiration, aquatic respiration and weathering. *Global Change Biology* **16**, 1966–1978. https://doi.org/10.1111/j.1365-2486.2009.02092.x.

IDEAM – Instituto de Hidrología, Meteorología y Estudios Ambientales 2017 *Atlas Climatologico de Colombia*. Unidad de planeacción minero energética (UPME), Ministerio de Ambiente, Vivienda y Desarrollo Territorial Instituto de Hidrología, Meteorología y Estudios Ambientales. Bogota, Colombia, p. 265.

IHA. 2010 *GHG Measurement Guidelines for Freshwater Reservoirs*. Derived from: the UNESCO/IHA Greenhouse Gas Emissions from Freshwater Reservoirs Research Project: International Hydropower Association (IHA), London, UK.

Integrated Environments. 2006 *Proyecto Hidroeléctrico Reventazón. Estudios Ambientales Adicionales. Parte I: Emisiones de Gases de Efecto Invernadero*. Environmental Resources Management (ERM) y Applied Aquatic Research Ltd, San José, Costa Rica.

Javadinejad, S., Dara, R. & Jafary, F. 2020 Climate change scenarios and effects on snow-melt runoff. *Civil Engineering Journal* **6** (9), 1715–1725. doi:10.28991/cej-2020-03091577.

Keller, M. & Stallard, R. F. 1994 Methane emission by bubbling from Gatun Lake, Panama. *Journal of Geophysical Research* **99**, 8307–8319. https://doi.org/10.1029/92jd02170.

Kemenes, A., Forsberg, B. R. & Melack, J. M. 2007 Methane release below a tropical hydroelectric dam. *Geophysical Research Letter* **34**, 1–5. https://doi.org/10.1029/2007gl029479.

Koprivnjak, J. F., Dillon, P. & Molot, L. 2010 Importance of CO_2 evasion from small boreal streams. *Global Biogeochemical Cycles* **24**, 1–9. https://doi.org/10.1029/2009gb003723.

Kumar, A. & Sharma, M. P. 2012 Greenhouse gas emissions from hydropower reservoirs. *Hydro Nepal Journal of Water Energy and Environment* **11**, 37–42. https://doi.org/10.3126/hn.v11i0.7159.

Lambert, M. & Fréchette, J. L. 2005 Analytical techniques for measuring fluxes of CO_2 and CH_4 from hydroelectric reservoirs and natural water bodies. *Greenhouse Gas Emissions Fluxes and Processes* 37–60. https://doi.org/10.1007/978-3-540-26643-3_3.

Li, S., Lu, X. & Bush, R. T. 2013 CO_2 partial pressure and CO_2 emission in the lower Mekong River. *Journal of Hydrology* **504**, 40–56. https://doi.org/10.1016/j.jhydrol.2013.09.024.

Lopera, L. M., Oviedo, L. M., Rodríguez, D. C., & Peñuela, G. A. 2016 Batch tests application for the determination of flows of methane and carbon dioxide in the degradation of plant material in the reservoir Topocoro. *Ingenierías USBMed* **7** (2), 67–73.

Lu, S., Dai, W., Tang, Y. & Guo, M. 2020 A review of the impact of hydropower reservoirs on global climate change. *Science of the Total Environment* **711**, 134996. https://doi.org/10.1016/j.scitotenv.2019.134996.

Mendonça, R., Barros, N., Vidal, L. O., Pacheco, F., Kosten, S. & Roland, F. 2012 Greenhouse gas emissions from hydroelectric reservoirs: what knowledge do we have and what is lacking? In: *Greenhouse gases – emission. Measurement and management*. chapter 3, pp. 55–79. https://doi.org/10.1023/B:CLIM.0000043158.52222.ee.

Obianyo, J. I. 2019 Effect of salinity on evaporation and the water cycle. *Emerging Science Journal* **3** (4), 255–262. http://dx.doi.org/10.28991/esj-2019-01188.

Ometto, J. P., Cimbleris, A. C., dos Santos, M. A., Rosa, L. P., Abe, D., Tundisi, J. G., Stech, J. L., Barros, N. & Roland, F. 2013 Carbon emission as a function of energy generation in hydroelectric reservoirs in Brazilian dry tropical biome. *Energy Policy* **58**, 109–116. https://doi.org/10.1016/j.enpol.2013.02.041.

Oo, H. T., Zin, W. W. & Thin Kyi, C. C. 2020 Analysis of streamflow response to changing climate conditions using SWAT model. *Civil Engineering Journal* **6** (2), 194–209. http://dx.doi.org/10.28991/cej-2020-03091464.

Qu, B., Aho, K. S., Li, C., Kang, S., Sillanpaa, M., Yan, F. & Raymond, P. 2017 Greenhouse gases emissions in rivers of the Tibetan Plateau. *Scientific Report* **7**, 16573. https://doi.org/10.1038/s41598-017-16552-6.

Richey, J. E., Melack, J. M., Aufdenkampe, A. K., Ballester, V. M. & Hess, L. L. 2002 Outgassing from Amazonian rivers and wetlands as a large tropical source of atmospheric CO_2. *Nature* **416**, 617–620. https://doi.org/10.1038/416617a.

Rocha, A. C., dos Santos, M. A., Lewis, J. E. & dos Santos, C. 2015 Emissions of greenhouse gases in terrestrial areas pre-existing to hydroelectric plant reservoirs in the Amazon: the case of Belo Monte hydroelectric plant. *Renewable and Sustainable Energy Reviews* **51**, 1728–1736. https://doi.org/10.1016/j.rser.2015.07.067.

Rosa, L. P., Schaeffer, R. & Santos, M. A. 1996 Are hydrolectric dams in the Brazilian Amazon significant sources of greenhouse gases?. *Environ. Conservation* **23** (1), 2–6.

Ruiz, M., Rodríguez, D. C., Chica, E. L. & Peñuela, G. A. 2019 Calibration of two mathematical models at laboratory scale for predicting the generation of methane and carbon dioxide at the entrance point of the Chucurí river to the Topocoro Reservoir, Colombia. *Ingeniería Y Competitividad* **21** (1), 11–22. https://doi.org/10.25100/iyc.v21i1.7651.

Soumis, N., Duchemin, É., Canuel, R. & Lucotte, M. 2004 Greenhouse gas emissions from reservoirs of the western United States. *Global Biogeochemical Cycles* **18**, 1–11. https://doi.org/10.1029/2003gb002197.

Sousa, I. L., Mannaerts, C. M., de Sousa, I. W., Barbosa, J. C., Verhoef, W., Fonseca, A. C. & Dantas, H. A. 2019 Conjunctive use of in situ gas sampling and chromatography with geospatial analysis to estimate greenhouse gas emissions of a large Amazonian hydroelectric reservoir. *Science of the Total Environment* **650** (1), 394–407. https://doi.org/10.1016/j.scitotenv.2018.08.403.

Takagaki, N. & Komori, S. 2007 Effects of rainfall on mass transfer across the air-water interface. *Journal of Geophysical Research* **112**, 148–227. https://doi.org/10.1029/2006JC003752.

Teodoru, C. R., Del Giorgio, P. A., Prairie, Y. T. & Camire, M. 2009 Patterns in pCO_2 in boreal streams and rivers of northern Quebec, Canada. *Global Biogeochemical Cycles* **23**, 1–11. https://doi.org/10.1029/2008GB003404.

Teodoru, C. R., Prairie, Y. T. & Del Giorgio, P. A. 2010 Spatial heterogeneity of surface CO_2 fluxes in a newly created Eastmain-1 reservoir in Northern Quebec, Canada. *Ecosystems* **14** (1), 28–46. https://doi.org/10.1007/s10021-010-9393-7.

Teodoru, C. R., Bastien, J., Bonneville, M. C., del Giorgio, P. A., Demarty, M., Garneau, M., Hélie, J. F., Pelletier, L., Prairie, Y. T., Roulet, N., Strachan, I. & Tremblay, A. 2012 The net carbon footprint of a newly created boreal hydroelectric reservoir. *Global Biogeochemical Cycles* **26**, 1–14. https://doi.org/10.1029/2011gb004187.

UNESCO/IHA. 2008 *GHG Measurement Guidelines for Freshwater Reservoirs. Prepared by the International Hydropower Association (IHA) in Collaboration with the International Programme (IHP) of the United Nations Educational*, Scientific and Cultural Organization (UNESCO), p. 17.

Valle, D. & Kaplan, D. 2019 Quantifying the impacts of dams on riverine hydrology under non-stationary conditions using incomplete data and Gaussian copula models. *Science of the Total Environment* **677**, 599–611. https://doi.org/10.1016/j.scitotenv.2019.04.377.

Wang, F., Wang, B., Liu, C. Q., Wang, Y., Guan, J., Liu, X. & Yu, Y. 2010 Carbon dioxide emission from surface water in cascade reservoirs-river system on the Maotiao River, southwest of China. *Atmospheric Environment* **45**, 3827–3834. doi:10.1016/J.ATMOSENV.2011.04.014.

First received 26 August 2021; accepted in revised form 17 December 2021. Available online 6 January 2022